

***Citation for the published version:***

Sáez-Trigueros, D., Hertlein, H., Meng, L., & Hartnett, M. (2016). Shape and Texture Combined Face Recognition for Detection of Forged ID Documents. In the 39th Intl. ICT (Information and Communication Technology) Convention MIPRO 2016 (pp. 1343). Croatia: IEEE. DOI: 10.1109/MIPRO.2016.7522348

***Document Version:*** Accepted Version

***Link to the final published version available at the publisher:***

<https://ieeexplore.ieee.org/document/7522348/>

© 2016 IEEE. Personal use of this material is permitted. Permission from IEEE must be obtained for all other uses, in any current or future media, including reprinting/republishing this material for advertising or promotional purposes, creating new collective works, for resale or redistribution to servers or lists, or reuse of any copyrighted component of this work in other works.

***General rights***

Copyright© and Moral Rights for the publications made accessible on this site are retained by the individual authors and/or other copyright owners.

Please check the manuscript for details of any other licences that may have been applied and it is a condition of accessing publications that users recognise and abide by the legal requirements associated with these rights. You may not engage in further distribution of the material for any profitmaking activities or any commercial gain. You may freely distribute both the url (<http://uhra.herts.ac.uk/>) and the content of this paper for research or private study, educational, or not-for-profit purposes without prior permission or charge.

***Take down policy***

If you believe that this document breaches copyright please contact us providing details, any such items will be temporarily removed from the repository pending investigation.

***Enquiries***

Please contact University of Hertfordshire Research & Scholarly Communications for any enquiries at [rsc@herts.ac.uk](mailto:rsc@herts.ac.uk)

# Shape and Texture Combined Face Recognition for Detection of Forged ID Documents

Daniel Sáez-Trigueros, Heinz Hertlein, Li Meng\*

School of Engineering and Technology  
University of Hertfordshire  
Hatfield AL10 9AB, UK

d.saez-trigueros@herts.ac.uk, L.I.MENG@herts.ac.uk

Margaret Hartnett

IDscan Biometrics Ltd  
London E14 9QD, UK

**Abstract**— This paper proposes a face recognition system that can be used to effectively match a face image scanned from an identity (ID) document against the face image stored in the biometric chip of such a document. The purpose of this specific face recognition algorithm is to aid the automatic detection of forged ID documents where the photography printed on the document's surface has been altered or replaced. The proposed algorithm uses a novel combination of texture and shape features together with subspace representation techniques. In addition, the robustness of the proposed algorithm when dealing with more general face recognition tasks has been proven with the Good, the Bad & the Ugly (GBU) dataset, one of the most challenging datasets containing frontal faces. The proposed algorithm has been complemented with a novel method that adopts two operating points to enhance the reliability of the algorithm's final verification decision.

**Keywords**—face recognition, shape and texture combined features, detection of forged IDs

## I. INTRODUCTION

Even though the first successful face recognition algorithms dated from the late eighties, it is still a vibrant area of research with new and better techniques appearing every year. One of the main reasons for the popularity of face recognition is the wide range of potential applications, including access control, identification systems, surveillance, and identity verification, to name but a few. This paper investigates the applicability of face recognition to the authentication of biometric ID documents, i.e., the process of analysing an ID document in order to prove its legitimacy. ID documents are specifically designed with security features (watermarks, holograms, special materials, etc.) to avoid counterfeiting and forgery. A counterfeit document is a complete reproduction of a document from scratch to resemble an officially issued document, whereas a forged document is a genuine document that has been illegally altered in some way.

Some organisations have studied how to detect fraudulent identity documents by examining their security features [1], [2]. This can be done manually by human operators, or automatically by processing the document electronically. In practice, the most effective method is a combination of both: documents are electronically validated and referred to a human operator when the automatic electronic validation fails for any reason. Nowadays, millions of ID documents are manually examined by human operators every day in different businesses and organisations. Thus, this study is motivated by the growing need for automatic or semi-automatic methods for authenticating ID documents.

This paper introduces an additional automatic validation check to detect forged documents by using face recognition for the comparison of the image printed on the ID document to the image stored in the ID document's biometric chip. This validation check aims to reduce one common method of forgery, namely photography substitution [1], [2].

The problem presented here is a specific face recognition case since it effectively compares whether the images themselves are identical (i.e. derived from the same camera shot). Hence, the main difficulties arise from the presence of watermarks, holograms, reflections and other imperfections on the scanned image as shown in Fig. 1. Other studies [3], [4] have investigated the problem of matching degraded face images scanned from passports to high-resolution digital face images. Those studies have proposed pre-processing methods to improve the quality of the scanned face images for their later use in a face recognition algorithm. While these pre-processing steps are likely to improve the overall performance, they are intrinsically domain specific. By not applying any domain specific pre-processing, the proposed algorithm is more generalised and can be used to compare any two face images. In order to test its accuracy for both the specific application considered here as well as more general face recognition applications, the proposed algorithm has been evaluated on two different datasets, namely (i) a proprietary dataset (hereinafter referred to as the BiometricID dataset) containing face images scanned from ID documents and digital images from the biometric chip of those documents; and (ii) the Good, the Bad & the Ugly (GBU) dataset, which contains pairs of frontal face images with three levels of difficulty [5].

The proposed face recognition method is based on the fusion of texture-based features and shape-based features. In particular, Scale-Invariant Feature Transform (SIFT) descriptors are used to extract the texture features, and a set of coefficients that represent relative distances between pairs of facial landmarks is used to describe the shape of the face. These two different types of features are further processed using Principal Component



Fig. 1. Example of image printed on an ID document (left) and image stored in the biometric chip of the same document (right).

Analysis (PCA) and Linear Discriminant Analysis (LDA) to project the features to a lower dimensional and more discriminating space. Furthermore, the use of two operating points is proposed to provide a greater degree of control over the verification decision.

The remainder of the paper is structured as follows. Section II provides a subject review with a focus on the approaches adopted in this study. Section III describes the proposed algorithm in detail and Section IV presents and analyses the experimental results. Finally, conclusions are drawn in Section V.

## II. SUBJECT REVIEW

### A. Face Alignment with Constrained Local Neural Field

The term face alignment is typically used in the literature to refer to the automatic detection of facial landmarks in a face image or video in order to support further processing. Those landmarks can be used to normalise faces to a canonical view using 2D or 3D transformations or to extract shape features out of the face image. The algorithm proposed in this paper makes use of the Constrained Local Neural Field (CLNF) algorithm [6], an extension of the Constrained Local Model (CLM) [7]. CLM and CLNF are based on the popular Active Appearance Model (AAM) method [8]. AAM is a statistical model of shape and texture created from a training set of manually annotated face images and subsequently used to fit new unseen images. The fitting process starts by placing landmark points on an image using the mean location of each landmark in the training set. Then, the texture residual between the current estimate and the model is calculated, and the shape parameters updated in order to minimise that residual. In both CLM and AAM methods, a set of rigid and non-rigid shape parameters  $\mathbf{p} = [s, \mathbf{R}, \mathbf{t}, \mathbf{q}]$  models the positions of the predefined set of landmarks

$$\mathbf{x} = s\mathbf{R}(\bar{\mathbf{x}} + \Phi\mathbf{q}) + \mathbf{t}, \quad (1)$$

where  $\mathbf{x}$  are the locations of the set of facial landmarks defining the face shape in the given image,  $\bar{\mathbf{x}}$  the mean shape of the faces in the training set,  $\Phi$  the principal component matrix describing the modes of variation among the face shapes and  $\mathbf{q}$  a vector of weights that control the non-rigid shape defined by  $\mathbf{x}$ . The rigid shape transformations are controlled by a scaling term  $s$ , a translation term  $\mathbf{t}$ , and a rotation matrix  $\mathbf{R}$ .

CLM methods offer better performance than AAM by using local descriptors to represent the texture surrounding each landmark location instead of utilising a global texture model of the whole face. The CLNF method, in particular, uses a local descriptor based on a neural network with one hidden layer and similarity and sparsity spatial constraints in the output to enhance the accuracy [6].

### B. Scale-Invariant Feature Transform

SIFT descriptors have been extensively used in object and face recognition [9]. The original SIFT algorithm [10] finds key points on an image and calculates a descriptor for each one of these key points. This section summarises how to calculate the descriptor. The process of finding the key points is not discussed here since the algorithm proposed in Section III calculates descriptors on fixed locations within the image.

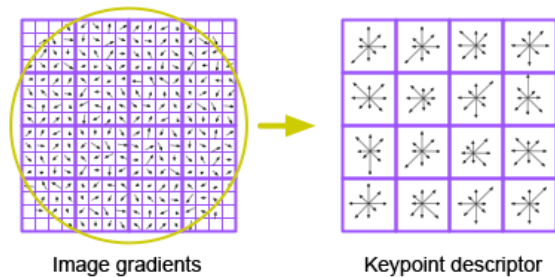


Fig. 2. Orientation histograms created from gradients sampled over a 16 x 16 region. The Gaussian weighting function is represented with a circular window on the left figure. Image taken from [11].

The first step is to compute gradients in a region of 16 x 16 pixels around the centre of the key point. Then, the magnitude of each gradient is weighted using a Gaussian weighting function to avoid abrupt changes in the descriptor and give less emphasis to gradients located far from the centre. Orientation histograms of 8 bins are then created using gradients within 4 x 4 sub regions. In an orientation histogram the bins can be represented by vectors pointing to different directions, where the length of each vector is the magnitude of the corresponding bin (see Fig. 2). The final descriptor is formed by concatenating the magnitudes of the bins of all the orientation histograms in the 16 x 16 region. Since there are 4 x 4 histograms, each containing 8 bins, the dimension of the descriptor is 128 [10].

### C. PCA and LDA in Face Recognition

The *Eigenfaces* algorithm based on PCA was one of the first successful face recognition techniques [12], and although its performance has since been surpassed by more advanced algorithms, PCA is still a relevant technique used in many modern face recognition algorithms. One of the limitations of PCA is that it does not use class labels, meaning that faces from the same identity and faces from different identities are treated in the same way.

LDA is a similar approach to PCA but uses the class (identity) labels to find a projection that minimises the variation within the classes while maximising the variation between classes, i.e., the identity labels are used to reduce intra-person variations while increasing inter-person variations. PCA is typically used before LDA to reduce the dimensionality of the input feature vector, as LDA does not perform well when the within-class scatter matrix is not well estimated. This happens when there are not enough samples in the training set compared to the high dimensionality of the input feature vector [13], [14]. This combination of PCA before LDA has been adopted in this work.

## III. PROPOSED ALGORITHM

### A. Face Normalisation

The Viola-Jones object detector [15] is applied to detect the position of the face(s) in a given image. In order to perform face alignment, the CLNF landmark detector is used to locate a set of 68 landmarks in each face [6]. Once the landmarks have been located, the positions of the pupils (which are found at the intersecting point defined by the landmarks surrounding the eye sockets) are used to normalise the face images to a common scale (128 x 128 pixels) and crop area, with the eyes located at fixed locations. Lastly, the image is converted to greyscale.

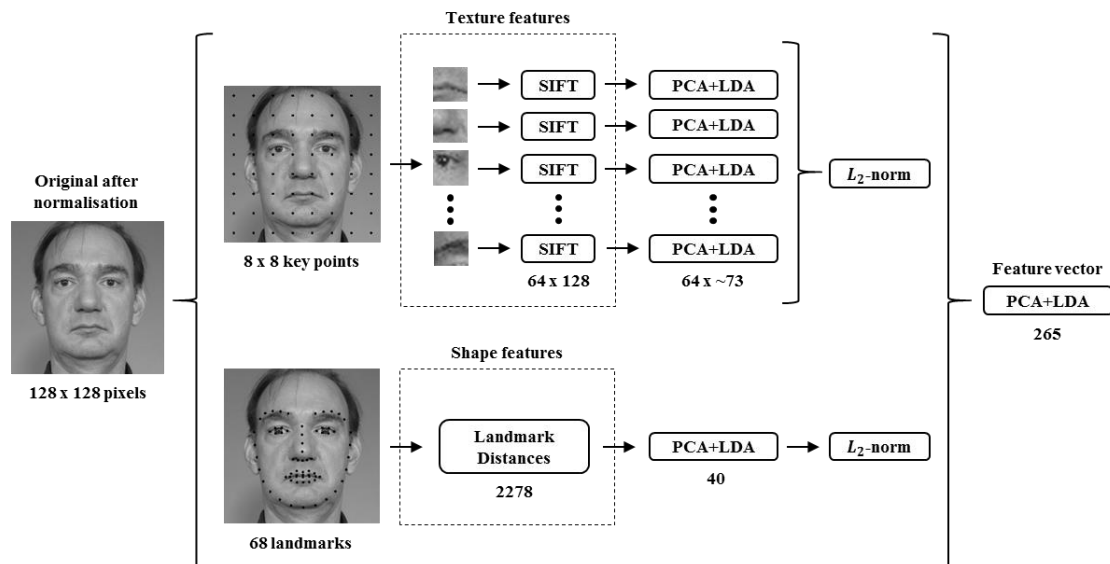


Fig. 3. Diagram illustrating the face representation step of the proposed algorithm. The figures below each block indicate the number of dimensions after each step.

## B. Face Representation

The face images are represented in two steps: firstly, a number of features are calculated to extract relevant information that are more informative than the raw pixels; secondly, the extracted features are transformed using machine learning techniques in order to create feature vectors that are more discriminating and, ideally, unique to each person.

### 1) Feature Extraction

Two different types of features are calculated in the proposed algorithm: texture-based features and shape-based features.

Texture features are the most popular kind of features for face recognition. They can represent more information than shape features as they are directly computed from the raw pixels. Shape features are usually calculated from landmark locations within the face image, which means that their reliability depends heavily on the accuracy of the landmark localisation algorithm. On the other hand, shape features can improve robustness in situations when the appearance of a face changes but not its geometry, for example, comparing face images of the same person with and without facial hair, makeup, or glasses. In this work, shape features are fused with texture features to boost the recognition accuracy of the proposed algorithm.

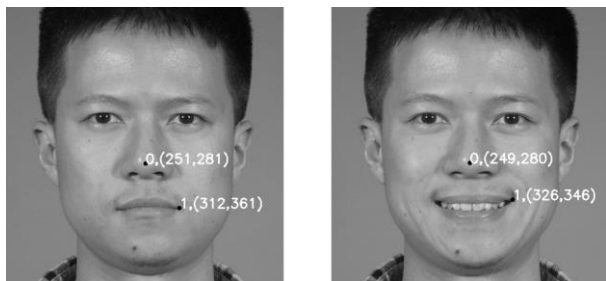


Fig. 4. The Euclidean distance between the highlighted landmarks when the expression is neutral (left image) is 100.60, and 101.41 when the expression is smiling (right image), i.e. the relative distance between the landmarks remains almost the same. On the other hand, the misalignment of the landmark in the right corner of the mouth when the person smiles is 20.52 with respect to the case in which the expression is neutral.

### a) Texture features

Inspired by [16], [17], the texture features used in the proposed algorithm consist of SIFT descriptors densely extracted from local patches across the face image. In particular, 64 SIFT descriptors with a radius of 6 pixels are extracted from a  $8 \times 8$  grid of fixed key points as shown in the top half of Fig. 2.

### b) Shape features

The shape features used in the proposed algorithm are Euclidean distances between pairs of landmarks. The distances are calculated after normalising the face image so that the effect of scaling is removed. The total number of possible distances is given by  $\binom{n}{2} = n(n-1)/2$ , where  $n$  is the total number of landmarks. As shown in the bottom half of Fig. 3, 68 landmarks are used resulting in a total number of landmark distances of 2,278.

Other studies have considered the use of landmarks for face representation. For example, the use of landmark coordinates and distances between pairs of landmarks has been studied in [18]. Their ratio-based model is very similar to the approach adopted in this paper. However, they made use of fewer landmark points and removed half of the distances due to the similarity between both sides of the face. In contrast, the approach adopted in this work uses all the possible landmark points to represent as much shape information as possible. In [19] the use of landmark locations for affine-invariant shape representation is studied. However, shape variations encountered in real datasets are not only a result of affine transformations but also of non-rigid transformations caused by, for example, changes in facial expression. As shown in Fig. 4 the shape features based on distances between pairs of landmarks are more robust to facial expressions than the shape features based on landmark locations.

### 2) Subspace Representation

Multivariate statistical tools can be used to transform a high dimensional space spanned by a large number of features into a lower dimensional space that retains the most useful information for discriminating the original samples.

As suggested in Section II.C, the proposed algorithm uses a common method in face recognition wherein LDA is applied to the subspace obtained by first applying PCA to the input data. In this work, PCA+LDA projections are used to independently transform the space spanned by each SIFT descriptor and the space spanned by the shape features. Other studies [17], [20], [21] have used a random sampling technique [22] to reduce the dimensionality of very high dimensional feature spaces (e.g. the space that would result from concatenating all the shape and texture features). However, independently applying PCA+LDA to lower dimensional spaces as proposed here has the advantage of eliminating the need of such random sampling techniques, which might otherwise accidentally remove highly discriminating features.

Using a PCA that retains 98% of the original variance, the 128-dimensional SIFT descriptors become (on average) 73-dimensional when the FRGC dataset is used for training (see Section IV.B), and the 2,278-dimensional vector representing the landmark distances becomes 40-dimensional. The observed significant reduction in dimensionality of both the texture and shape vectors, notwithstanding the retention of 98% of the variance in the data, substantiates the notion that many distances between pairs of landmarks must be highly correlated as they are calculated from landmarks being located next to each other.

The next step is to combine the shape and texture features. First, all the PCA+LDA projected texture features are concatenated resulting in a 4,670-dimensional vector ( $64 \times \sim 73$ ) and normalised to unit  $L_2$ -norm. The PCA+LDA projected shape features are normalised in the same way prior to being concatenated with the texture features. The feature vector resulting from concatenating the shape and texture features is 4,710-dimensional (4,670 texture features and 40 shape features) and might contain redundant information. For this reason, another PCA+LDA transformation is performed to project the information contained in the concatenated texture and shape features into a more discriminating feature space with even lower dimensionality. In this case a PCA retaining 90% of the variance is performed to reduce the dimensionality to 265 before applying LDA. A diagram describing the entire face representation step is depicted in Fig. 2.

Another way of fusing multiple modalities such as face texture and shape is to have separate recognition algorithms for each modality and then combine their scores [19]. However, feature-level fusion has the advantage of having to train a single algorithm, and eliminates the need to optimise the fusion weighting. Liu and Wechsler [23] used a feature-level fusion method similar to the one proposed here. However, the input features in [23] are the raw image pixels and the landmark coordinates instead of the more informative features considered in this study.

### C. Face Matching

In this work, the matching score between two feature vectors  $\mathbf{a}$  and  $\mathbf{b}$  is calculated using the cosine similarity:

$$\cos(\mathbf{a}, \mathbf{b}) = \frac{\mathbf{a} \cdot \mathbf{b}}{\|\mathbf{a}\| \|\mathbf{b}\|} \quad (2)$$

Typically, the operating point of the algorithm is determined by a threshold  $t$  used to decide whether two face images match or not. This threshold defines the true and the false acceptance rates (TAR and FAR) and the true and the false rejection rates (TRR and FRR). When analysing such a conventional biometric system that operates with one threshold only, the verification accuracy is completely specified by the pair of error rates FAR and FRR, as  $\text{TAR} = 1 - \text{FRR}$  and  $\text{TRR} = 1 - \text{FAR}$ . As shown in Fig. 5, with one threshold and one operating point, FRR can be reduced arbitrarily at the expense of increasing FAR and vice versa.

In order to alleviate the conflict between FRR and FAR, an approach that uses two thresholds, i.e., two operating points, is adopted here. In this approach, the higher threshold  $t_h$  controls the accepted comparisons (TAR and FAR), whereas the lower threshold  $t_l$  controls the rejected comparisons (TRR and FRR). A matching score in between the two operating points would yield an undetermined result. As shown in Fig. 6, this approach allows both FRR and FAR to be reduced at the same time, as they are determined separately by two different thresholds. In real applications, it is often desirable to achieve very low error rates whilst it is acceptable to have a certain number of undetermined cases, which might be handled further in a specific way (e.g. by manual inspection). Therefore, the introduction of a second threshold represents a significant improvement in terms of the applicability of face verification in practice.

## IV. EXPERIMENTAL RESULTS

This section presents details about the protocol and the datasets adopted for the evaluation of the proposed algorithm (Section IV.A), the subsets used for training (Section IV.B), and the evaluation results (Section 0).

### A. Evaluation Protocol and Datasets

The protocol adopted for the evaluation of the algorithm is based on the protocol as defined by NIST for its face recognition challenges [24]. In this protocol, the algorithms are tested by comparing all the images in a target set to all the images in a query set. The resulting scores are used to generate a Receiver Operating Characteristic (ROC) curve that plots TAR against FAR.

The proposed algorithm is evaluated on two different datasets. The BiometricID set is a proprietary database where for each subject there are face images scanned from his/her ID document (i.e. scanned images with artifacts such as watermarks, holograms, etc.), and the original digital face image obtained from the biometric chip of the same ID document (i.e. the RFID image). For some subjects there are more than one scanned images (as the artifacts can vary from one scan to the next), and some others do not have any scanned or RFID image. In such cases, all the images are used to form additional matching or non-matching pairs. For example, if a subject only has one scanned image and no RFID image, the scanned image is compared against all the RFID images in the evaluation set to produce extra non-matching pairs. In total, the target set contains 4,802 RFID images and the query set 8,801 scanned images forming 6,029 matching pairs and 42,256,373 non-matching pairs.

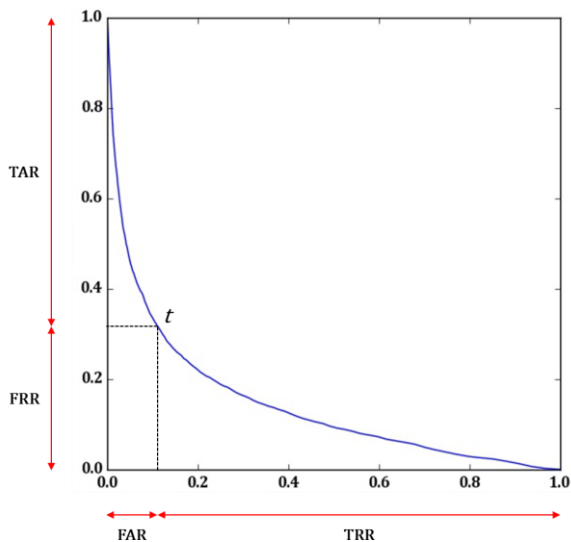


Fig. 5. ROC curve plotting FAR against FRR and a possible threshold. It can be seen the effect that increasing or decreasing the threshold  $t$  has on TAR, FRR, FAR and TRR.

The second database is the Good, the Bad and the Ugly public dataset [5], one of the most challenging sets available to evaluate the performance of face recognition algorithms on frontal images. The GBU dataset is divided into three partitions. The Good partition consists of face pairs easy to match, the Bad partition consists of face pairs with an average matching difficulty and the Ugly partition consists of face pairs difficult to match. The query and target sets of each partition contain 1,085 images from 437 subjects. The distribution of images on each query and target set, i.e., the number of images per subject, is the same across the three partitions. In total, there are 3,297 matching pairs and 1,179,928 non-matching pairs on each partition.

### B. Training

Two different sets of images have been used to train the algorithm, one for each dataset evaluated in this study. One is a random subset of the BiometricID dataset for evaluation on the BiometricID dataset, and the other is a random subset of the FRGC dataset [25] for evaluation on the GBU dataset. Since the GBU dataset does not provide training images, the FRGC dataset is used as both of them contain images that were collected by the University of Notre Dame under similar conditions.

The BiometricID training set contains 1,000 images from 500 subjects, with 2 images per subject, one RFID image and one scanned image. Only 2 images per subject are used since any additional sample available for a subject is simply a different scan of the face image printed on the ID document. The training set used for evaluating the algorithms on the GBU dataset contains 5,320 images of a total of 266 subjects from the FRGC dataset with 20 images per subject. Recognition of face images on the BiometricID dataset is considerably easier than recognition on the GBU dataset in the sense that the algorithm requires less training data to perform well on the BiometricID dataset. This is because for the face images in the BiometricID dataset the PCA+LDA only needs to learn feature vectors to match two different versions of the same face image (RFID and scanned) and differentiate them from feature vectors generated for face images of other subjects; whereas the more general scenario presented by the GBU dataset requires similar (matching) feature

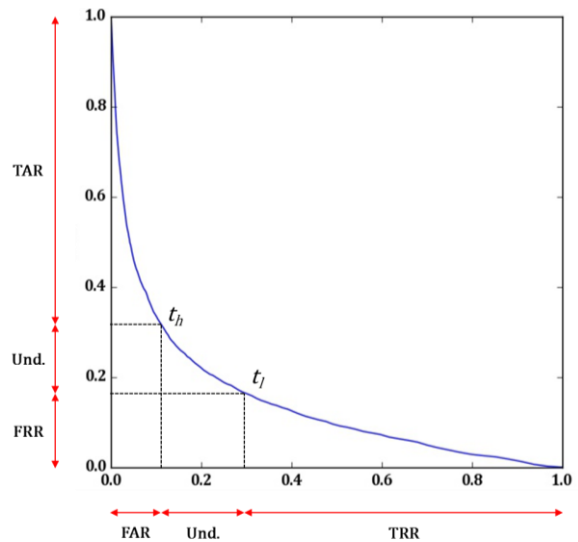


Fig. 6. ROC curve plotting FAR against FRR and two possible thresholds. In comparison with Fig. 4, the introduction of the lower threshold  $t_l$  allows to reduce FRR at the expense of reducing TRR and having comparisons where the result is undetermined. In real applications this is often desirable, as the number of comparisons between non-matching faces is usually much lower than the number of comparisons between matching faces.

vectors generated for various, and sometimes dramatically different, face images of each and every subject in the dataset.

### C. Results

The open source implementation of the 4SF algorithm described in [16] has been chosen as the baseline for the performance evaluation in this work. The 4SF algorithm is a good example that makes use of local descriptors and subspace representation. To focus the comparison on the face recognition accuracy rather than on the face detection accuracy, the same face alignment technique has been adopted in both algorithms. For this reason, the 4SF algorithm was modified to use the CLNF landmark detector to locate the position of the eye pupils. Moreover, the 4SF algorithm is trained and evaluated using exactly the same images as the proposed algorithm.

As seen in the ROC curves obtained with the BiometricID dataset (Fig. 7) and the GBU dataset (Fig. 8), the proposed algorithm outperforms the baseline algorithm in all cases. This implies that (i) the proposed combination of texture and shape features possesses more discriminating information than texture features alone (at least when evaluating datasets that contain mainly frontal images), and (ii) the proposed PCA+LDA applied to multiple low dimensional spaces is a more effective dimensionality reduction strategy than the random sampling technique used in 4SF.

## V. CONCLUSIONS

This paper presents a novel face recognition algorithm tailored for a specific application scenario of face recognition that involves face images with added security features such as watermarks and holograms for the detection of forged ID documents.

Considering the similar face geometry across faces of the same subject, the proposed algorithm fuses face shape features with the commonly used face texture features. The high dimensionality produced by the large number of shape and texture

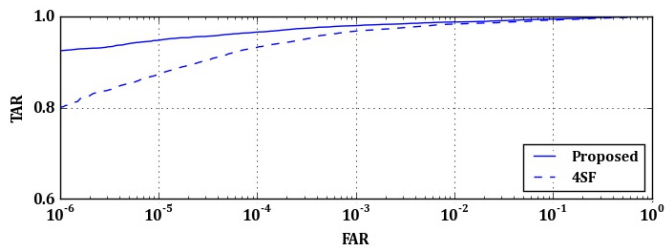


Fig. 7. ROC curves on the BiometricID dataset using the 4SF algorithm and the proposed algorithm.

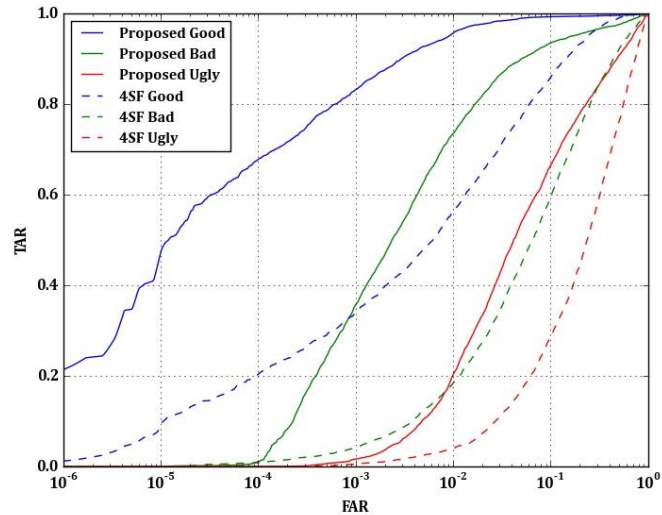


Fig. 8. ROC curves on the Good, Bad and Ugly partition of GBU dataset using the 4SF algorithm and the proposed algorithm.

features has been avoided by using multiple PCA+LDA transforms. The proposed algorithm has achieved high accuracy for the specific application scenario considered here. In addition, the robustness of the proposed algorithm for more generic face recognition tasks has been confirmed by its performance on the GBU dataset, offering a good balance between training and accuracy in the sense that there is no need to train using many thousands of images as is the case with the latest face recognition algorithms based on deep learning [26].

Finally, it has been shown how the applicability of any face recognition algorithm in real applications can be benefited with the use of two thresholds to have a better control on the face recognition rates at the expense of having comparisons where the result is undetermined.

## REFERENCES

- [1] 'Guidance on Examining Identity Documents'. UK Home Office, 18-Nov-2014.
- [2] 'A Good Practice Guide On Pre-Employment Screening - Document Verification'. Centre for the Protection of National Infrastructure (CPNI), Jun-2007.
- [3] T. Bourlai, A. Ross, and A. Jain, 'On matching digital face images against scanned passport photos,' in *Proc. First IEEE Int. Conf. Biometrics, Identity and Security (BIDS)*, 2009.
- [4] T. Bourlai, A. Ross, and A. K. Jain, 'Restoring Degraded Face Images: A Case Study in Matching Faxed, Printed, and Scanned Photos,'

- IEEE Trans. Inf. Forensics Secur.*, vol. 6, no. 2, pp. 371–384, Jun. 2011.
- [5] P. J. Phillips *et al.*, 'An introduction to the good, the bad, & the ugly face recognition challenge problem', in *IEEE Int. Conf. Automatic Face & Gesture Recognition and Workshops*, 2011, pp. 346–353.
- [6] T. Baltrušaitis, P. Robinson, and L.-P. Morency, 'Constrained local neural fields for robust facial landmark detection in the wild,' in *IEEE Int. Conf. Computer Vision Workshops (ICCVW)*, 2013, pp. 354–361.
- [7] D. Cristinacce and T. F. Cootes, 'Feature Detection and Tracking with Constrained Local Models,' 2006, pp. 95.1–95.10.
- [8] T. F. Cootes, G. J. Edwards, and C. J. Taylor, 'Active appearance models,' *IEEE Trans. Pattern Anal. Mach. Intell.*, vol. 23, no. 6, pp. 681–685, Jun. 2001.
- [9] M. Bicego, A. Lagorio, E. Grosso, and M. Tistarelli, 'On the Use of SIFT Features for Face Authentication,' in *Conf. Computer Vision and Pattern Recognition Workshop*, 2006, pp. 35–35.
- [10] D. G. Lowe, 'Distinctive image features from scale-invariant keypoints,' *Int. J. Comput. Vis.*, vol. 60, no. 2, pp. 91–110, 2004.
- [11] 'Computer Vision Project'. [Online]. Available: <http://www.cc.gatech.edu/~hays/compvision/results/proj2/rchawla8/index.html>. [Accessed: 05-Jan-2016].
- [12] M. A. Turk and A. P. Pentland, 'Face recognition using eigenfaces,' in *IEEE Conf. Computer Vision and Pattern Recognition*, 1991, pp. 586–591.
- [13] W. Zhao *et al.*, 'Discriminant Analysis of Principal Components for Face Recognition,' in *Face Recognition*, Springer Berlin Heidelberg, 1998, pp. 73–85.
- [14] P. N. Belhumeur, J. P. Hespanha, and D. J. Kriegman, 'Eigenfaces vs. fisherfaces: Recognition using class specific linear projection,' *IEEE Trans. Pattern Anal. Mach. Intell.*, vol. 19, no. 7, pp. 711–720, 1997.
- [15] P. Viola and M. J. Jones, 'Robust real-time face detection,' *Int. J. Comput. Vis.*, vol. 57, no. 2, pp. 137–154, 2004.
- [16] J. C. Klontz *et al.*, 'Open source biometric recognition,' in *IEEE Conf. Biometrics: Theory, Applications and Systems (BTAS)*, 2013, pp. 1–8.
- [17] Z. Li, U. Park, and A. K. Jain, 'A Discriminative Model for Age Invariant Face Recognition,' *IEEE Trans. Inf. Forensics Secur.*, vol. 6, no. 3, pp. 1028–1037, Sep. 2011.
- [18] J. Shi, A. Samal, and D. Marx, 'How effective are landmarks and their geometry for face recognition?' *Comput. Vis. Image Underst.*, vol. 102, no. 2, pp. 117–133, May 2006.
- [19] T. Wu, P. Turaga, and R. Chellappa, 'Age Estimation and Face Verification Across Aging Using Landmarks,' *IEEE Trans. Inf. Forensics Secur.*, vol. 7, no. 6, pp. 1780–1788, Dec. 2012.
- [20] B. Klare and A. K. Jain, 'Face recognition across time lapse: On learning feature subspaces,' in *Int. Joint Conf. Biometrics*, 2011, pp. 1–8.
- [21] B. F. Klare *et al.*, 'Face Recognition Performance: Role of Demographic Information,' *IEEE Trans. Inf. Forensics Secur.*, vol. 7, no. 6, pp. 1789–1801, Dec. 2012.
- [22] X. Wang and X. Tang, 'Random Sampling for Subspace Face Recognition,' *Int. J. Comput. Vis.*, vol. 70, no. 1, pp. 91–104, Oct. 2006.
- [23] C. Liu and H. Wechsler, 'A shape-and texture-based enhanced Fisher classifier for face recognition,' *IEEE Trans. Image Process.*, vol. 10, no. 4, pp. 598–608, 2001.
- [24] S. Rizvi, J. Phillips, and H. Moon, 'The FERET verification testing protocol for face recognition algorithms,' in *Proc. Third IEEE Int. Conf. Automatic Face and Gesture Recognition*, 1998, pp. 48–53.
- [25] N. US Department of Commerce, 'Face Recognition Grand Challenge (FRGC)'. [Online]. Available: <http://www.nist.gov/itl/iad/ig/frgc.cfm>. [Accessed: 04-Aug-2015].
- [26] Y. Taigman, M. Yang, M. Ranzato, and L. Wolf, 'Deepface: Closing the gap to human-level performance in face verification,' in *IEEE Conf. Computer Vision and Pattern Recognition (CVPR)*, 2014, pp. 1701–1708.